

Low-temperature electronic transport properties in thin films of Pd and PdH_{0.3}

E. Flouda and C. Papastaikoudis

Institute for Materials Science, National Center for Scientific Research, "Democritos," GR-153 10 Agia Paraskevi, Attiki, Athens, Greece

(Received 28 December 1993; revised manuscript received 13 June 1994)

Low-temperature magnetoresistance measurements have been used to determine various electron scattering times in pure Pd and PdH_{0.3} thin films with different thicknesses, which have been prepared by electron-gun evaporation. From low-field magnetoresistance measurements, using localization theory, the spin-flip, electron-electron, and electron-phonon relaxation times can be deduced and they are found to depend on the electronic structure of both systems. It is also found that the increase of the disorder of the systems enhances the spin-orbit coupling, which is larger in PdH_{0.3} than in Pd. On the other hand, the high-field magnetoresistance allows the determination of both the Coulomb screening factor F and the Landé factor g for both systems. It is found that the F factor depends on the band structure and takes the mean values 0.63 and 0.53 for pure Pd and PdH_{0.3}, respectively, while the g factor depends on the degree of disorder.

I. INTRODUCTION

During recent years theoretical and experimental investigations of the transport properties of the electrons in two-dimensional metallic systems have revealed two new quantum effects, namely, the weak localization of electrons^{1,2} and the enhancement of electron-electron interaction in the presence of impurity scattering.³⁻⁶ The weak localization is due to the fact that at low temperatures the phase coherence of the electron wave function is preserved over the characteristic length $L_\varphi = (D\tau_\varphi)^{1/2}$ which is equal to the electron diffusion length within the phase relaxation time τ_φ , where D is the diffusion coefficient. In the electron-electron interaction the characteristic length is the interaction length $L_T = (\hbar D / k_B T)^{1/2}$, where k_B is the Boltzmann constant. The interelectron interaction at finite values of the electron mean free path l leads to the appearance of a correction on both the electron density of states on the Fermi level and on the conductivity. Both effects predict that in two-dimensional systems and at low temperatures the conductivity decreases logarithmically as the temperature decreases. The magnitude of the decrease, as predicted by weak localization and electron-electron interaction, is of the same order. It follows then that measurements of the temperature dependence of the conductivity do not suffice to distinguish the two effects.

The existence of a magnetic field applied perpendicularly to the film plane allows one to separate localization and electron-electron interaction effects. A magnetic field destroys localization and generally causes a negative magnetoresistance. When spin-orbit effects are taken into account the magnetoresistance can change sign.

Taking into account both spin-orbit and magnetic impurity spin scattering Hikami, Larkin, and Nagaoka⁷ have calculated the correction of the magnetoresistance via the relation

$$\frac{\delta R_\square(T, H)}{R_\square^2} = \zeta \left\{ \psi \left[\frac{1}{2} + \frac{H_1}{H} \right] - \psi \left[\frac{1}{2} + \frac{H_2}{H} \right] + \frac{1}{2} \left[\psi \left[\frac{1}{2} + \frac{H_3}{H} \right] - \psi \left[\frac{1}{2} + \frac{H_4}{H} \right] \right] \right\}, \quad (1)$$

where R_\square is the sheet resistance, $\zeta = e^2 / 2\pi^2 \hbar = 1.23 \times 10^{-5} \Omega^{-1}$, ψ is the digamma function, H is the applied field, and $H_1 - H_4$ are characteristic fields which are defined as

$$\begin{aligned} H_1 &= H_{el} + H_{so} + H_s, \\ H_2 &= H_4 = \frac{4}{3}H_{so} + \frac{2}{3}H_s + H_{in}, \\ H_3 &= H_\varphi = 2H_s + H_{in}. \end{aligned} \quad (2)$$

H_{el} , H_{in} , H_s , and H_{so} are due to elastic or potential scattering, inelastic scattering, magnetic scattering, and spin-orbit scattering, respectively. H_φ is the phase-breaking field.

The characteristic fields H_x are connected to the relaxation times τ_x by the relation

$$H_x = \frac{\hbar}{4eD\tau_x}, \quad (3)$$

where D is the diffusion constant. The relationship between the diffusion lengths L_x and the corresponding relaxation times τ_x is given by $L_x = (D\tau_x)^{1/2}$.

On the other hand, the contribution of the electron interaction effects to magnetoresistance is small. Lee and Ramakrishnan⁸ have shown that the particle-hole diffusion channel causes a splitting of the spin-up and spin-down bands when a magnetic field H is applied. This splitting produces a gap of the order of $g\mu_B H$ be-

tween the lowest unoccupied spin-up electron and the highest occupied spin-down ones. g is the Landé factor of conduction electrons and μ_B the Bohr magneton. The magnetoresistance due to this splitting is given in two-dimensions by⁸

$$\frac{\Delta R_{\square}(T, H)}{R_{\square}^2} = \xi \left[\frac{\tilde{F}}{2} \right] 0.084h^2 \quad (4a)$$

for $h \ll 1$, where $h = g\mu_B H/kT$ and

$$\frac{\Delta R_{\square}(T, H)}{R_{\square}^2} = \xi \left[\frac{\tilde{F}}{2} \right] \ln \left[\frac{h}{1.3} \right] \quad (4b)$$

for $h \gg 1$. \tilde{F} is the two-dimensional effective electron screening constant and is given by⁹

$$\tilde{F} = 8(1 + F/2)\ln(1 + F/2)/F - 4, \quad (5)$$

where F is the general screening factor which is given by the relation¹⁰

$$F = \frac{K}{\pi(1 - K^2)^{1/2}} \ln \left[\frac{1 + (1 - K^2)^{1/2}}{1 - (1 - K^2)^{1/2}} \right], \quad (6)$$

$K = (2k_F/\kappa)^{-1}$, where k_F is the Fermi wave vector and κ^{-1} is the screening length in three dimensions:

$$\kappa^{-1} = \left[\frac{N(\epsilon_F)e^2}{\epsilon_0} \right], \quad (7)$$

$N(\epsilon_F)$ is the density of states at Fermi level. The screening factor F approaches 1 for strong screening and 0 for weak screening.

According to Eqs. (1), (4a), and (4b) the weak localization in the case of strong spin-orbit scattering as well as the electron-electron interaction effect predict that the magnetoresistance exhibits the same field dependence. Although it is nearly impossible to distinguish the two effects only from magnetoresistance measurements, it is, however, possible to calculate the important parameters which are involved in these two mechanisms.

The present investigation deals with the study of the magnetoresistance change occurring in thin films of pure Pd and PdH_x in α and β phase, in which hydrogen is located interstitially in the octahedral sites of the fcc Pd lattice.

The aim of this work is to study the influence of the modification of the electronic band structure by weak localization and interaction effects, to calculate the important parameters which are involved in these two theories and finally to compare the present results with earlier investigations.¹¹

As discussed by Raffy *et al.*,¹¹ pure Pd is a d metal with a high density of states at Fermi energy, while the PdH_x system with $x = 0.3$ is a normal metal with an electronic structure similar to that of a noble s - p metal with a much lower Fermi-level density of states. Raffy *et al.*¹¹ have studied the magnetoresistance of PdH_x thin films with $x > 0.7$ and have shown how the electronic structure can be influenced by both weak localization and electron-electron interaction and how these two effects interplay with a cooperative phenomenonlike supercon-

ductivity. Recently, the present authors^{12,13} by simultaneous measurements of the Hall coefficient and magnetoresistance in Pd and PdH_{0.3} thin films have found that (i) localization and interaction effects coexist, and (ii) the screening factor F in hydrogenated system is reduced compared to that in Pd.

II. EXPERIMENTAL PROCEDURE

Five Pd films were prepared in an ultrahigh vacuum chamber ($\sim 10^{-9}$ mbar) by electron-beam evaporation. The films were deposited onto a quartz substrate at room temperature with a rate of about 2 Å/s. The thickness which ranged from 50 to 380 Å was measured during the evaporation with a quartz crystal oscillator calibrated with a stylus profilometer (DEKTAK IIA).

The pure films were first measured and afterwards were charged with hydrogen from the gas phase at room temperature as it is described elsewhere.¹² The hydrogen concentration was measured during both absorption and desorption and was controlled to be about $x = 0.3$ for all films.

The measurements were carried out in a conventional stainless-steel helium cryostat equipped with a superconducting solenoid with a maximum field strength of 6 T. The resistance measurements were performed by means of a four-terminal dc technique with the sample voltage amplified by a photoelectric galvanometer and then displayed on an HP 3435 A digital multimeter. To avoid sample heating the currents used did not exceed 1 mA. All measurements were performed in the temperature range 1.8–4.2 K.

III. RESULTS AND DISCUSSION

The values of the sheet resistance $R_{\square} = \rho/d$ of the investigated pure Pd and PdH_x films as well as other parameters are listed in Table I. Table I shows that the sheet resistances R_{\square} of the pure Pd films are slightly higher than those of hydrogenated system. This difference can be attributed, as mentioned above, to the fact that these two systems have different electronic band structures. Although the strong scattering of the s electrons on the d states is absent in the PdH_x system, it dominates in pure Pd. In Fig. 1 the resistivity ρ of both

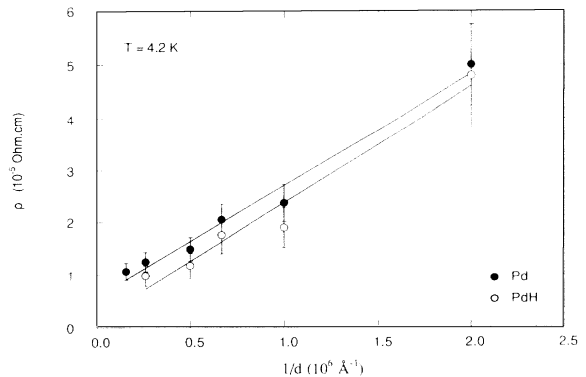


FIG. 1. The electrical resistivity ρ of pure Pd and PdH_{0.3} alloys as a function of the inverse thickness d^{-1} .

TABLE I. Sample characteristics for pure Pd and PdH_{0.3} thin films.

Thickness (Å)	$R_{\square\text{Pd}}(4.2\text{ K})$ (Ω/□)	$R_{\square\text{PdH}_{0.3}}(4.2\text{ K})$ (Ω/□)	$D(\text{Pd})$ ($\times 10^{-4}$ m ² /s)	$D(\text{PdH}_x)$ ($\times 10^{-4}$ m ² /s)
380	3.3	2.6	11.5	34.1
200	7.4	5.9	9.6	28.6
150	13.7	11.7	7.0	19.2
100	23.7	19.0	6.1	17.8
50	100	96.0	2.9	7.0

systems is plotted as a function of inverse thickness d^{-1} at 4.2 K. The figure shows that ρ is a nearly linear function of $1/d$, i.e., ρ follows the Fuchs law¹⁴

$$\rho = \rho_B \left[1 + \frac{3l_B}{8d} \right]. \quad (8)$$

Here ρ_B and l_B are the resistivities and the electron free paths of the bulk systems, respectively. The solid lines are least-square fitted to Eq. (8) with ρ_B and l_B as the fitting parameters. The fitted values of the product $\rho_B l_B$ are $5.68 \times 10^5 \Omega \text{Å}^2$ and $5.94 \times 10^5 \Omega \text{Å}^2$ for pure Pd and PdH_{0.3} thin films, respectively. The validity of Fuchs law means that the present Pd and PdH_{0.3} films are clean, homogeneous, and the mean-free path of the electrons is essentially controlled by the thickness d . Table I also presents the electron-diffusion coefficients for both systems as it is calculated via the relation

$$D = [e^2 N(\epsilon_F) \rho]^{-1} = [e^2 N(\epsilon_F) d R_{\square}]^{-1}, \quad (9)$$

where ρ is the resistivity, R_{\square} the sheet resistance, and d the film thickness. The density of states $N(\epsilon_F)$ at ϵ_F for pure Pd and for PdH_{0.3} systems are $N(\epsilon_F) = 2.71 \times 10^{47} \text{J}^{-1} \text{m}^{-3}$ and $6.07 \times 10^{46} \text{J}^{-1} \text{m}^{-3}$, respectively.¹⁵

Figures 2 and 3 show the transverse magnetoresistance ($2\pi^2 \hbar / e^2 \Delta R_{\square} / R_{\square}^2(0)$) of the pure Pd and PdH_{0.3} systems, respectively, as a function of the magnetic field for the thin film with a thickness of 100 Å and at the fixed temperatures 2, 3, and 4.2 K; all the other samples show nearly identical data. The main features of these results are that (i) the magnetoresistance of both systems is positive, as has been observed by other authors,^{10,11,16–18} and

(ii) the magnetoresistance of the PdH_{0.3} system is lower than that of the pure Pd one. The latter feature is in contradiction to the results of Raffy *et al.*¹¹ The cause of this discrepancy is due to both the different method of the films loading and to the different hydrogen concentration. The films under discussion here were loaded from the gas phase at room temperature, and were in the $\alpha + \beta$ phase at the measuring temperatures, while the films discussed by Raffy *et al.*¹¹ were charged at low temperatures by an electrochemical process and were in the pure β phase.

From the present measurements of the magnetoresistance in Pd and PdH_{0.3} films it can be inferred that an interpretation of the data in terms of only one mechanism is impossible. In order to distinguish the two mechanisms we consider the data of the magnetoresistance in two magnetic-field regions, i.e., in the low-field and in the high-field regions.

A. Low magnetic-field region

At low magnetic fields the electron-electron interaction contribution is expected to be negligible and thus one need consider only the weak localization effect. The experimental data can then be fitted using the theoretical expression given by Eq. (1).

The characteristic field $H_{\text{el}} = \hbar / 4eD\tau_{\text{el}} = \hbar v_F / 4eDl_{\text{el}}$ arising from the elastic scattering, with $D = 7 \times 10^{-4} \text{m}^2/\text{s}$, $v_F = 0.3 \times 10^8 \text{cm/s}$,¹⁹ and $l_{\text{el}} = 150 \text{Å}$, is of the order of about 3 T. Since H_{el} is considerably larger than the applied field H the term $\psi(\frac{1}{2} + H_1/H)$ in Eq. (1) con-

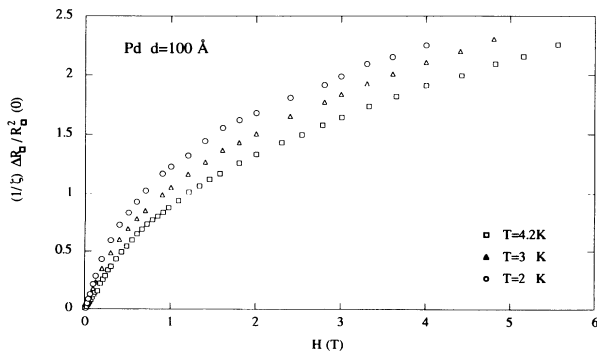


FIG. 2. The transverse magnetoresistance of the pure Pd film 100 Å in thickness as a function of the magnetic field H .

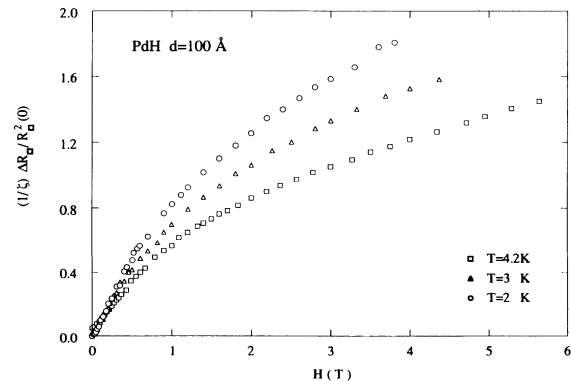


FIG. 3. The transverse magnetoresistance of the PdH_{0.3} film 100 Å in thickness as a function of the magnetic field H .

tributes little to the magnetoresistance and can be ignored. In this case, Eq. (1) should be replaced by

$$\frac{\delta R_{\square}(T, H)}{R_{\square}^2} = \zeta \left[-\frac{3}{2} \psi \left(\frac{1}{2} + \frac{H_2}{H} \right) + \frac{1}{2} \psi \left(\frac{1}{2} + \frac{H_3}{H} \right) \right] \quad (10)$$

Equation (10) holds up to a magnetic field $H_E \approx 2$ T. Up to this value no discrepancy between the theoretical and experimental points can be observed.

The solid curves fitted to the experimental data in Figs. 4(a)–4(e) are derived from relation (10) using a suitable fitting program and the characteristic fields H_2 and H_3 as adjustable parameters. The agreement between the experimental points and the theory is very good. The parameter H_3 is equal to the characteristic phase-breaking field H_{φ} . In Figs. 4(a)–4(e) the values H_{φ} are plotted as a

function of the temperature T for four Pd films, in both the pure and the hydrogenated state. From these figures one can see the following features. First, $H_{\varphi}(\text{Pd}) > H_{\varphi}(\text{PdH}_{0.3})$ for the sample with a thickness of 380 Å, while for thinner films there is a certain temperature T_{α} below which $H_{\varphi}(\text{Pd}) < H_{\varphi}(\text{PdH}_{0.3})$. This cross-over temperature T_{α} shifts to higher values as the thickness decreases. The other feature to note is that the dephasing field H_{φ} can be separated into two parts, the first is temperature independent, while the second is temperature dependent.

The solid lines of Figs. 4(a)–4(e) are the best fits described by the temperature dependence

$$H_{\varphi} = 2H_s + H_{in}(T) = C + BT + AT^3 \quad (11)$$

The constant term C can be identified with the charac-

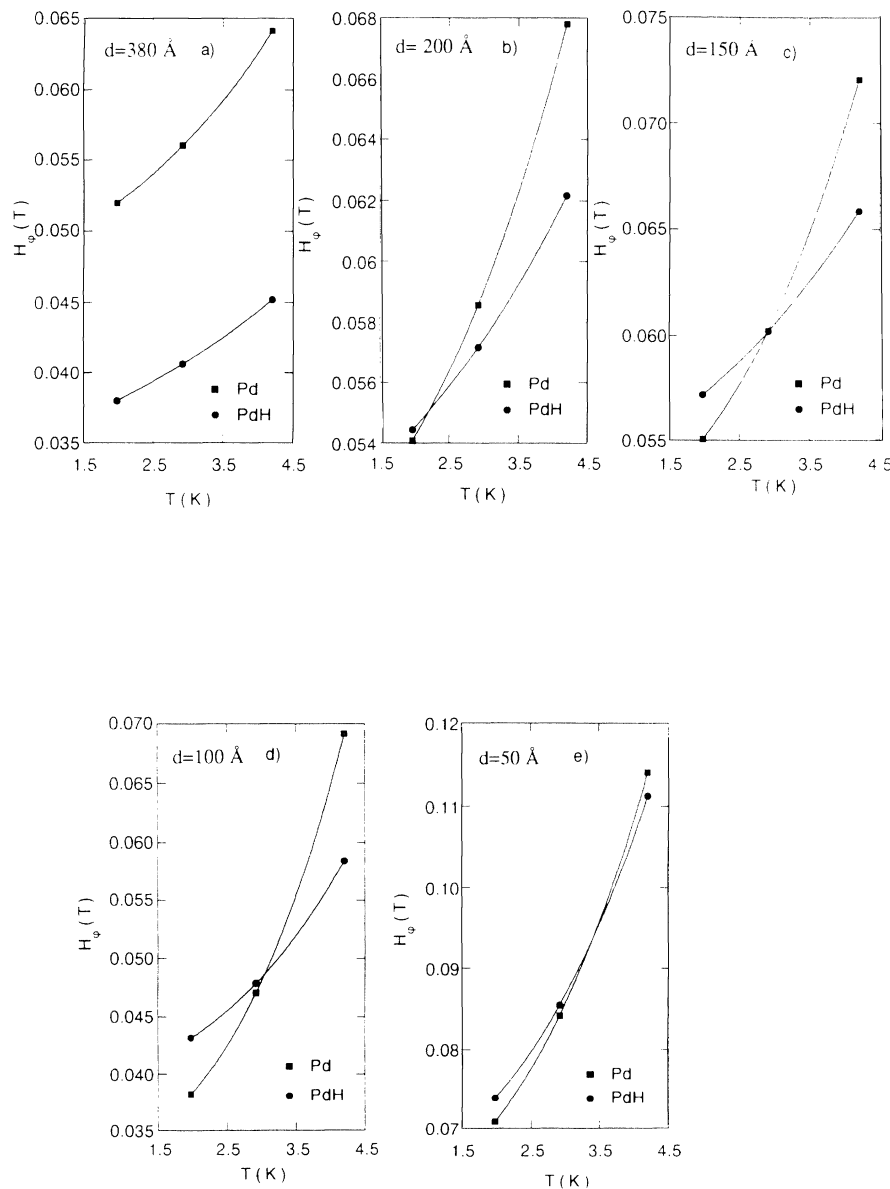


FIG. 4. The phase-breaking field H_{φ} as a function of temperature T for pure Pd and PdH_{0.3} thin films.

teristic field $2H_s$, responsible for the spin-flip scattering due to the presence of residual magnetic impurities, while the terms BT and AT^3 correspond to the contribution to the characteristic inelastic magnetic field H_{in} .

The obtained C values are presented in Table II. Note that C or, similarly, H_s decreases with d . According to Lin and Giordano²⁰ the origin of the spin-flip scattering should be attributed to reasons other than the substrate impurities, since the quartz substrates contain minor magnetic impurities (< 3 ppm).

According to the same authors the decrease of H_s with d can be explained if one assumes that the spin-flip scattering occurs predominantly at the film surface. As the film thickness decreases the ratio surface to volume becomes larger and the surface scattering becomes more probable and more important.

Note also that the H_s values of the pure films are smaller than those of the hydrogenized ones. Raffy *et al.*¹¹ suggest that this behavior can be attributed to the d character of Pd. H_s is mainly affected by the d impurities. It seems then reasonable that the influence of these impurities is smaller in a d metal, such as Pd, than in an s - p , one, such as PdH.

The BT and AT^3 terms of Eq. (11) are due to impurity-induced scattering,^{21,22} and electron-phonon scattering,²³ respectively. The relevant inelastic scattering rate τ_{in}^{-1} , which corresponds to the characteristic field H_{in} can then be written as

$$\tau_{in}^{-1} = \tau_{ee}^{-1} + \tau_{ep}^{-1} = B^*T + A^*T^3. \quad (12)$$

The thin films investigated here are considered to be two-dimensional and in the dirty limit, with respect to the electron-electron scattering, because the thermal diffusion length $L_T = (\hbar D / k_B T)^{1/2}$ for all films is larger than the thickness d in the whole temperature range (1.8–4.2 K). For a dirty two-dimensional system Abrahams *et al.*²¹ have calculated τ_{ee}^{-1} and found that

$$\tau_{ee}^{-1} = \frac{e^2}{2\pi\hbar^2} R_{\square} k_B T \ln(T_1/T), \quad (13)$$

where $T_1 = 1.85 \times 10^5 (k_F l_{el})^3 K \sim 10^{12} K$, l_{el} is the elastic scattering length and k_F the Fermi wave vector. As $T_1 \gg T$ and $\ln(T_1/T) \sim 27$, expression (13) leads to a linear T dependence, i.e.,

$$\tau_{ee}^{-1} = 13.7 \times 10^7 R_{\square} T = B^*T \quad (14a)$$

or

$$H_{ee} = \frac{\hbar}{4eD} 13.7 \times 10^7 R_{\square} T = 2.25 \times 10^{-8} \frac{R_{\square}}{D} = B_{th} T. \quad (14b)$$

The experimental magnitudes B presented in Table II are in good agreement with the relevant theoretical predictions, which are also included in the same table.

An additional criterion for the dimensionality of the present films is the phonon propagation. The dimensionality of a system with respect to electron-phonon scattering is generally decided²³ by comparing the thickness of the system to the most probable phonon wavelength, $\lambda_{ph} = \hbar v_s / 2k_B T$, where v_s is the velocity of the sound. The electron-phonon scattering rate shows a T^3 dependence in both the clean three-dimensional limit, i.e., $l, d > \lambda_{ph}$, and the dirty two-dimensional limit, i.e., $l, d < \lambda_{ph}$, while the clean two-dimensional limit exhibits a T^2 dependence. In pure Pd, transverse phonons give the major contribution to the inelastic scattering. Taking $v_s = 2.63 \times 10^5$ cm/s,¹⁰ it is found that $\lambda_{ph} \approx 630 \text{ \AA} / T$, where T is the temperature in K. Thus, in the temperature range 1.8–4.2 K, λ_{ph} varies from 350 to 150 \AA. Therefore, with respect to the phonons the present films are in the intermediate dimensionality between two and three. The fact that the films are in direct contact to the quartz substrate enhances the three-dimensionality because the phonons extend into the quartz, despite a mismatch at the interface. In this case the electron-phonon scattering rate is given by the relation²³

$$\tau_{e-ph}^{-1} = 14\pi\zeta(3)\lambda\omega_D \left(\frac{T}{\Theta_D} \right)^3 = A_{th}^* T^3 \quad (15a)$$

or

$$H_{e-ph} = \frac{\hbar}{4eD} 14\pi\zeta(3)\lambda\omega_D \left(\frac{T}{\Theta_D} \right)^3 = A_{th} T^3, \quad (15b)$$

where ω_D and Θ_D are the Debye frequency and temperature, respectively, λ is the electron-phonon coupling parameter and $\zeta(3)$ is the three-dimensional Riemann function. Taking for both Pd and PdH_{0.3} a mean value of 270 K for the Debye temperature Θ_D (Ref. 24) and $\omega_D = 3.54 \times 10^{13} \text{ s}^{-1}$, while $\lambda_{Pd} = 0.45$ (Ref. 25) and $\lambda_{PdH_x} \approx 0.26$ for concentrations $x \leq 0.73$,²⁴ the A_{th} values can be calculated. The results are listed in Table II. The values of A_{exp} listed in the same table are to be compared to the values of A_{th} obtained by fitting the ex-

TABLE II. Theoretical and experimental parameters for pure Pd and PdH_{0.3} alloys.

Coefficient d (\AA)	B_{th} ($\times 10^{-4}$ T/K)		B_{exp} ($\times 10^{-4}$ T/K)		A_{th} ($\times 10^{-4}$ T/K ³)		A_{exp} ($\times 10^{-4}$ TK ³)		C ($\times 10^{-4}$ T)	
	Pd	PdH	Pd	PdH	Pd	PdH	Pd	PdH	Pd	PdH
380	0.60	0.16	1.95	1.70	7.8×10^{-2}	0.66×10^{-2}	1.0	0.37	400	333
200	1.61	0.43	2.60	2.05	9.3×10^{-2}	0.78×10^{-2}	1.2	0.48	480	500
150	4.07	1.27	4.28	2.27	0.13	1.17×10^{-2}	1.8	0.52	492	522
100	8.08	2.22	12.8	9.70	0.15	1.26×10^{-2}	3.9	1.64	307	380
50	71.70	28.53	60.4	55.0	0.31	3.20×10^{-2}	4.5	3.80	554	600

perimental data to Eq. (11) up to the magnetic field $H_E \approx 2$ T.

As mentioned above the temperature-dependent part of the dephasing field $H_\varphi(T)$ is larger in pure Pd than in $\text{PdH}_{0.3}$, i.e., $H_{\text{in}}(\text{Pd}) > H_{\text{in}}(\text{PdH}_{0.3})$, particularly for the thicker samples. In order to explain this observation the electron-electron and electron-phonon scattering have to be considered separately. Raffy *et al.*¹¹ suggest that electron-electron scattering in pure Pd films, just as in the bulk state, is enhanced by the scattering of the *s* conduction electrons on the *d* states. As a result the scattering rate is multiplied by a factor of the order $[1 + N_d(\epsilon_F)/N_s(\epsilon_F)]$, where $N_d(\epsilon_F)$ and $N_s(\epsilon_F)$ are the *d* and the *s* densities of states at the Fermi energy, respectively. According to the same authors¹¹ a second mechanism which can also enhance the scattering rate in pure Pd is the scattering of the *s* electrons on the localized fluctuations of the *d*-band electron spin density. This scattering process contributes a T^2 dependence to the

low-temperature resistivity.

As far as the electron-phonon scattering rate $[\tau_{e\text{-ph}}]^{-1}$ is concerned, it is found to be greater in pure Pd than in $\text{PdH}_{0.3}$. The difference can be attributed to the different values of the electron-phonon coupling parameter λ . Theoretical calculations of the λ parameter for pure Pd (Ref. 25) give a value $\lambda = 0.45$, while for the PdH_x system the λ parameter is given by summing the contributions of each atom, namely $\lambda_{\text{PdH}_x} = \lambda_{\text{Pd}} + \lambda_{\text{H}}$. Using self-consistent augmented plane-wave (APW) band-structure calculations, Papaconstantopoulos *et al.*²⁶ determined the coupling constants of PdH_x alloys. They found that the value λ_{Pd} of Pd in PdH_x , 0.175, does not vary significantly with *x*, while the λ_{H} of H in PdH_x shows a strong concentration dependence, decreasing substantially as the hydrogen concentration decreases. According to Fig. 5 and Table IV of Ref. 26 it seems that the total value of the coupling parameter in PdH_x for $x < 0.73$ is

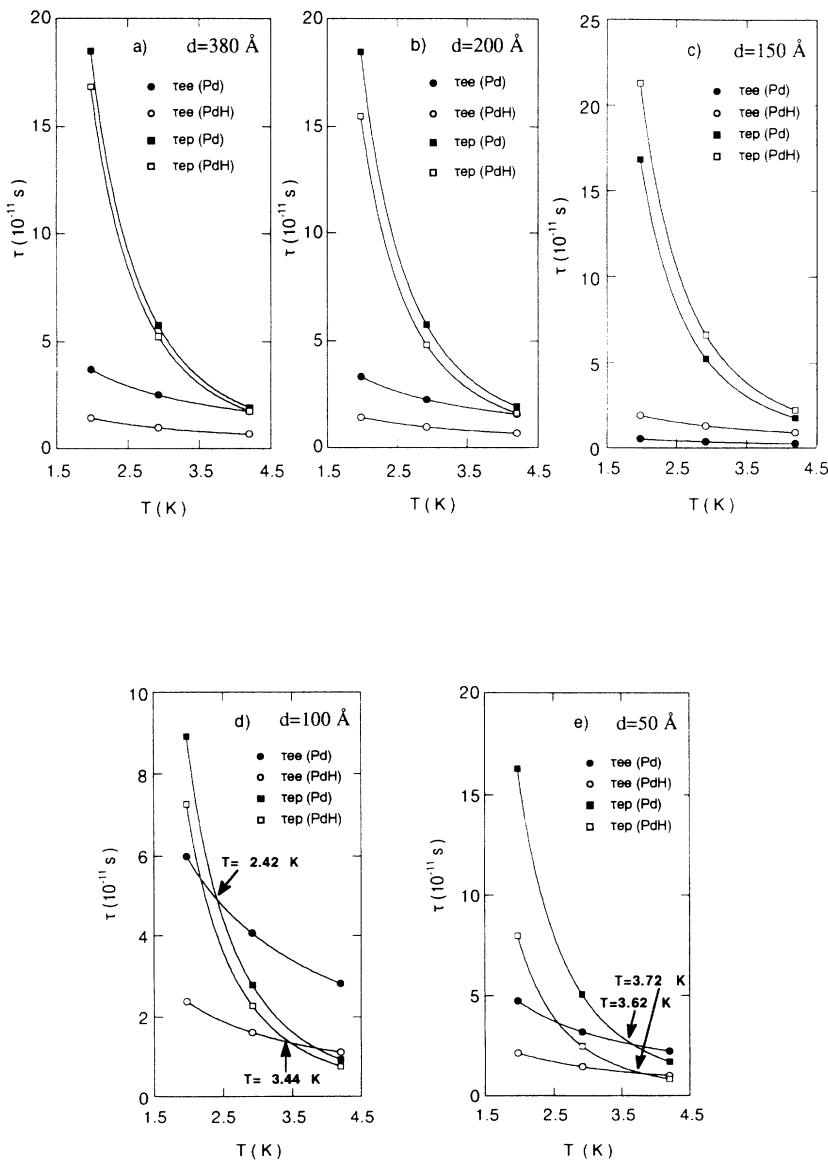


FIG. 5. The relaxation times τ_{e-e} and τ_{e-ph} as a function of temperature T for pure Pd and $\text{PdH}_{0.3}$ thin films.

nearly constant and amounts to $\lambda_{\text{tot}} \approx 0.26$. The corresponding λ_H value of H in PdH_x amounts to $\lambda_H \approx 0.085$. Therefore the calculation shows that the electron-phonon coupling constant λ_{pd} in pure Pd is a factor of 2 larger than the λ_{pd} in palladium hydride. The physical origin of this λ difference can be attributed to the s - d scattering mechanism, which takes place in pure Pd.

Figures 5(a)–5(e) show the relaxation times τ_{e-e} and τ_{e-p} as a function of the temperature T for the pure as well as for the hydrogenated films. The solid lines are the best fitted to Eqs. (14b), and (15b), using the values of parameters A_{exp} and B_{exp} in place of A_{th} and B_{th} . From this figure one can notice that (i) $(\tau_{e-e}, \tau_{e-p})_{\text{Pd}} > (\tau_{e-e}, \tau_{e-p})_{\text{PdH}_{0.3}}$ and (ii) $(\tau_{e-p})_{\text{Pd}, \text{PdH}_{0.3}} > (\tau_{e-e})_{\text{Pd}, \text{PdH}_{0.3}}$ for the thicker films (380–150 Å) in the whole temperature range, while for the thinner films (100–50 Å) there is a temperature T_α above which the relation $(\tau_{e-p})_{\text{Pd}, \text{PdH}_{0.3}} < (\tau_{e-e})_{\text{Pd}, \text{PdH}_{0.3}}$ is valid. As is mentioned elsewhere,¹³ below T_α the electron-phonon interaction is frozen out, while simultaneously, localization is suppressed. These two effects permit the observation of electron-electron interactions.

B. Spin-orbit scattering

The second parameter that can be determined by the fitting process to the experimental data of the transverse magnetoresistance using Eq. (1) is the characteristic field $H_2 = \frac{4}{3}H_{\text{so}} + \frac{2}{3}H_s + H_{\text{in}}$. Having previously obtained the characteristic fields H_s and H_{in} it is further possible to adjust the characteristic field H_{so} , which represents the strength of the spin-orbit scattering. The results of the H_{so} , values as well as the associated values of the spin-orbit scattering rate τ_{so}^{-1} and the elastic scattering rate τ_0^{-1} for Pd and $\text{PdH}_{0.3}$ thin films are shown in Table III. The elastic-scattering rate τ_0^{-1} has been evaluated from the relation $l_{\text{el}} = v_F \tau_0$, where the elastic mean-free path l_{el} is taken equal to the thickness d and v_F , the Fermi velocity, and is equal to 0.3×10^8 cm/s (Ref. 19) and 0.7×10^8 cm/s (Ref. 19) for pure Pd and PdH_x , respectively. Table III also shows the ratio τ_0/τ_{so} . In Fig. 6 the values of τ_{so}^{-1} are plotted as a function of the inverse film thickness d^{-1} for both systems. This figure shows that τ_{so}^{-1} increases in both systems and τ_{so}^{-1} in $\text{PdH}_{0.3}$ is about a factor of 2 larger than that of pure Pd. This means that the dissolved hydrogen enhances the spin-orbit coupling. On the other hand, the ratio τ_0/τ_{so} is nearly constant in both systems, with values between 7×10^{-3} and 1.4×10^{-2} . In comparison to the present localization experiments

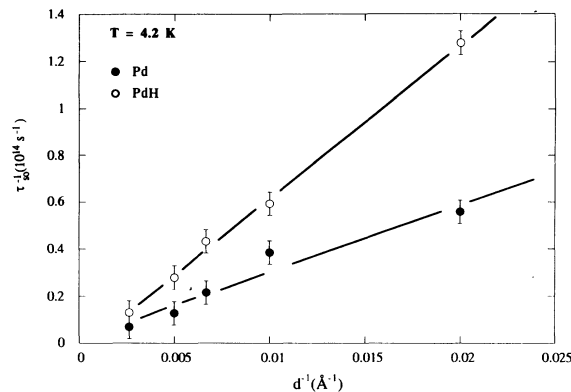


FIG. 6. The spin-orbit relaxation rate τ_{so}^{-1} as a function of the inverse thickness d^{-1} for pure Pd and $\text{PdH}_{0.3}$ thin films.

Meservey and Tedrow,²⁷ on previous critical field studies on superconductive PdH_x films 50–250 Å in thickness, have obtained values of τ_0/τ_{so} between 9×10^{-4} and 1.5×10^{-3} , i.e., an order of magnitude lower than the present measurements. The present τ_0/τ_{so} ratio is in rather good agreement with the ratio calculated from the Abrikosov and Gorkov relation:²⁸

$$\frac{\tau_0}{\tau_{\text{so}}} = (\alpha Z)^4, \quad (16)$$

where $\alpha = e^2/\hbar c$ is the fine-structure constant and Z is the atomic number. Equation (16) predicts $\tau_0/\tau_{\text{so}} = 1.3 \times 10^{-2}$ if one uses $Z = 46$ for Pd.

The fact that the ratio τ_0/τ_{so} is nearly constant in both systems suggests that the spin-orbit scattering arises from the same events in both of them. The mechanism which seems to be responsible for the spin-orbit scattering in the disordered films in the scattering of the Bloch wavefunctions from deviations in the periodicity of the lattice.²⁹ This deviation becomes stronger as the film thickness decreases. Therefore, the spin-orbit coupling should also increase as the thickness decreases. On the other hand, the dissolved interstitial hydrogen atoms occupy octahedral sites in the fcc Pd. Below about 300°C the homogeneous solid solution disintegrates into the α phase with low hydrogen content and an expanded β phase. The lattice of the β phase, when it is built up by discontinuous expansion of the α phase, is highly distorted.³⁰ This additional disorder, which is caused by the existence of the β phase, is responsible for the observed enhanced spin-orbit coupling.

TABLE III. The fitted fields H_{so} , τ_{so}^{-1} , τ_0^{-1} , and τ_0/τ_{so} for pure Pd and $\text{PdH}_{0.3}$ alloys.

d (Å)	H_{so} ($\times 10^{-2}$ T)		τ_{so}^{-1} ($\times 10^{13}$ s $^{-1}$)		τ_0^{-1} ($\times 10^{13}$ S $^{-1}$)		τ_0/τ_{so} ($\times 10^{-1}$)	
	Pd	PdH	Pd	PdH	Pd	PdH	Pd	PdH
380	0.98	0.63	0.68	1.30	0.77	1.85	8.8	7.0
200	2.19	1.60	1.28	2.78	1.49	3.57	8.6	7.8
150	3.17	3.71	1.35	4.35	2.00	4.76	6.8	9.1
100	10.4	5.50	3.84	5.88	3.03	7.14	12.7	8.2
50	31.7	38.7	5.58	12.82	5.88	14.00	9.5	9.2

C. High magnetic fields

As mentioned above, there is a fixed magnetic field H_E above which there is a difference between the experimental results and the theoretical curve given by Eq. (10). In order to supply the theoretical expression with a positive term the electron-electron interaction contribution should be taken into account. In this case the term given by Eq. (4b) should be added,

$$\left[\frac{\Delta R_{\square}(T, H)}{R_{\square}^2} \right]_{ee} = \zeta \left[\frac{\tilde{F}}{2} \right] \ln \left[\frac{h}{1.3} \right],$$

where $h = g\mu_B H/kT = \alpha_{ee}/T$. Fitting the high magnetic-field magnetoresistance data, for $H > H_E$, one can obtain \tilde{F} and α_{ee} for pure Pd and PdH_{0.3}. From the values of \tilde{F} and α_{ee} one can obtain the screening factor F and the Landé factor g of electron. The results are presented in Table IV. Table IV values show that the screening factor F in pure Pd is generally larger than that in PdH_{0.3}, while the F factor in both systems is nearly constant. The mean values of F in Pd and PdH_{0.3} are $F(\text{Pd}) \approx 0.63$ and $F(\text{PdH}_{0.3}) \approx 0.53$. These values are in good agreement with previous Hall effect measurements.^{12,13} The theoretical values of F calculated from Eq. (6) are $F(\text{Pd})_{\text{th}} = 0.58$ and $F(\text{PdH}_x)_{\text{th}} = 0.41$, using as density of states the values $N(\text{Pd}) = 2.71 \times 10^{47} \text{ J}^{-1} \text{ m}^{-3}$ and $N(\text{PdH}_x) = 6.07 \times 10^{46} \text{ J}^{-1} \text{ m}^{-3}$, respectively. The agreement between F_{exp} and F_{th} is found to be good within the experimental errors. It is obvious that for all the films the relation $F(\text{Pd}) > F(\text{PdH}_{0.3})$ is valid. The change of the screening factor as a result of the dissolution of hydrogen means that the screening length varies. In comparison, Markiewicz and Rollins¹⁷ found that F varies between 0.1 and 0.26 for Pd-Si and Pd/Pd-Si films with thicknesses between 55 and 30 Å, respectively. The difference between the values of F for pure Pd reported here and those of Markiewicz and Rollins¹⁷ may be attributed to both different fitting processes and data analysis. Markiewicz and Rollins obtained F values by fitting simultaneously the parallel and perpendicular data in the whole magnetic range (0–14 T), while the present F values were obtained by fitting the perpendicular magnetoresistance data above the threshold field $H_E > 2$ T. During the present fitting process the localization parameters were obtained by the low-field fitting, and they were afterwards kept constant, while the electron-electron interaction parameters were varied to obtain the best fit of

TABLE IV. The screening factor F and the Landé factor g for pure Pd and PdH_{0.3} alloys.

d (Å)	F		g	
	Pd	PdH	Pd	PdH
380	0.78	0.40	2.5	1.7
200	0.70	0.69	2.3	1.6
150	0.55	0.48	1.8	1.5
100	0.47	0.45	1.7	1.4
50	0.72	0.53	1.5	1.3

the high-field data. Finally, the localization parameters were also allowed to vary to get the best minimum of the fitting routine.

From the fitting parameter α_{ee} the Landé factor g can be obtained for Pd and PdH_{0.3} thin films. The values of g factor are presented in Table IV. This Table shows that the Landé factor values are different from the free-electron value $g_e = 2$, depending on the film thickness, and are lower in the PdH_{0.3} system. Figure 7 shows the g factors as a function of the thickness d in both systems. This figure shows that the g factor depends nearly linearly on the thickness d and in the two thicker pure Pd films has values larger than the free-electron value $g_e = 2$. On the other hand, the values for the PdH_{0.3} system are smaller than g_e . For comparison to the present values for the pure Pd thin films, the dashed line of Fig. 7 shows the g' factor for bulk Pd samples, which is measured at room temperature with a modified magnetomechanical method and is found to take the value 1.77.³¹ The dotted curve in the same figure shows the spectroscopic splitting g'' factor which is measured by the transmission electron resonance method,³² and has an average value of 2.25. Band-structure calculations have found average values for the g factor over the Fermi surface which lie between 2.22 and 2.31.^{33,34} These values are in good agreement with the present values. It should be mentioned that the present value is in large disagreement with the value of $g = 14$ of pure Pd thin films obtained by Markiewicz and Rollins¹⁷ from the same kind of measurements. Markiewicz and Rollins¹⁷ attributed the large g value they found to the modification of the band structure due to the lower film dimensionality or to many-electron effects.

In order to interpret both the dependence of the g factor on the film thickness and the influence of hydrogen on g values, spin-orbit coupling and its dependence on the disorder should be taken into account. As mentioned above, the increase of disorder by the reduction of the thickness, as well as by the introduction of hydrogen, strengthens the spin-orbit coupling. This enhancement of

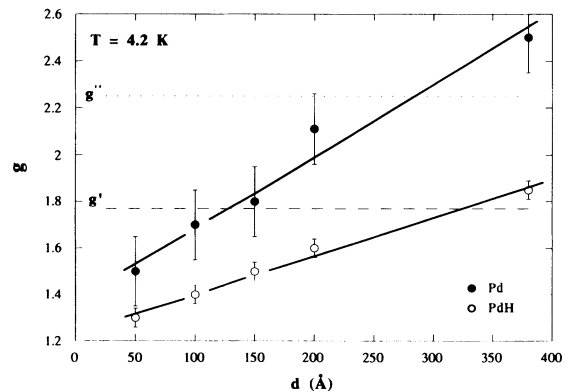


FIG. 7. The g factors as a function of the thickness d of the pure Pd and PdH_{0.3} thin films. The dashed and dotted lines correspond to the magnetomechanical g' and to the spectroscopic splitting g'' Landé factor of bulk Pd, respectively.

spin-orbit coupling causes a reduction of the g factor. According to Mueller *et al.*,³⁵ the reduction of the effective g factor in Pd from 2.00 to 1.65 can be explained by the presence of strong d -state spin-orbit coupling. Since the spin-orbit rate τ_{so}^{-1} depends linearly on the d^{-1} , according to the above arguments the g factor should change as a function of d . When hydrogen is dissolved in Pd, it causes more disorder in the thin-film lattice, as well as stronger spin-orbit coupling, in such a way that the g factor of the hydride is lower than that of pure Pd. On the other hand, electron-spin-resonance measurements in PdH alloys³⁶ containing Mn^{2+} and Gd^{3+} ions have shown that the H^+ ions do not participate in the spin-orbit scattering. The lower g values for the $PdH_{0.3}$ system cannot be attributed to either the band-structure modification or to the change of the Fermi energy ϵ_F since, in those cases, the g factor should have been thickness independent.

IV. CONCLUSION

In the present investigation we have attempted, by low-temperature measurements of the magnetoresistance of pure Pd and $PdH_{0.3}$ thin films, to understand the inelastic-scattering mechanisms that destroy the phase coherence, which is essential for localization, and to determine both the screening factor F and the spectroscopic splitting factor g , which are involved in the electron-electron interaction. From the low-field magnetoresistance measurements the three-dimensional electron-phonon and the two-dimensional electron-electron rates were obtained, and it has been concluded that the spin-orbit coupling depends on the strength of the disorder. From the high-field magnetoresistance measurements the screening factor F and the Landé factor g have been estimated. F takes the mean value 0.63 for pure Pd and 0.53 for $PdH_{0.3}$, while the g factor depends on the spin-orbit coupling.

- ¹E. Abrahams, P. W. Anderson, D. C. Licciardello, and T. V. Ramakrishnan, *Phys. Rev. Lett.* **42**, 673 (1979).
- ²P. W. Anderson, E. Abrahams, and T. V. Ramakrishnan, *Phys. Rev. Lett.* **43**, 718 (1979).
- ³B. L. Altshuler, A. G. Aronov, and P. A. Lee, *Phys. Rev. Lett.* **44**, 1288 (1980).
- ⁴B. L. Altshuler, D. Khmel'nitzkii, A. I. Larkin, and P. A. Lee, *Phys. Rev. B* **22**, 5142 (1980).
- ⁵H. Fukuyama, *J. Phys. Soc. Jpn.* **48**, 2169 (1980).
- ⁶H. Fukuyama, *J. Phys. Soc. Jpn.* **50**, 3407 (1981).
- ⁷S. Hikami, A. I. Larkin, and Y. Nagaoka, *Prog. Theor. Phys.* **63**, 707 (1980).
- ⁸P. A. Lee and T. V. Ramakrishnan, *Rev. Mod. Phys.* **57**, 287 (1985); *Phys. Rev. B* **26**, 4009 (1982).
- ⁹A. M. Finkelstein, *Zh. Eksp. Teor. Fiz.* **84**, 168 (1983) [*Sov. Phys. JETP* **57**, 97 (1983)].
- ¹⁰W. C. McGinnis and P. M. Chaikin, *Phys. Rev. B* **32**, 6319 (1985).
- ¹¹H. Raffy, P. Nédellec, L. Dumoulin, D. S. McLachlan, and J. P. Burger, *J. Phys.* **46**, 627 (1985); H. Raffy, L. Dumoulin, P. Nédellec, and J. P. Burger, *J. Phys. F* **15**, L37 (1985).
- ¹²E. Flouda and C. Papastaikoudis, *Z. Phys. Chem.* **181**, 921 (1993).
- ¹³E. Flouda, A. Travlos, and C. Papastaikoudis, *Solid State Commun.* **85**, 895 (1993).
- ¹⁴K. Fuchs, *Proc. Cambridge Philos. Soc.* **34**, 100 (1938).
- ¹⁵A. C. Switendick, in *Hydrogen in Metals I*, edited by G. Alefeld and J. Völkl, *Topics in Applied Physics* Vol. 28 (Springer-Verlag, Berlin, 1978), p. 101.
- ¹⁶W. C. McGinnis, M. J. Burns, R. W. Simon, G. Deutscher, and P. M. Chaikin, *Physica* **107B**, 5 (1981).
- ¹⁷R. S. Markiewicz and C. J. Rollins, *Phys. Rev. B* **29**, 735 (1984).
- ¹⁸L. Dumoulin, H. Raffy, P. Nédellec, D. S. McLachlan, and J. P. Burger, *Solid State Commun.* **51**, 85 (1984).
- ¹⁹D. A. Papaconstantopoulos, in *Metal Hydrides*, Vol. 76 of *NATO Advanced Study Institute, Series B: Physics*, edited by G. Bambakidis (Plenum, New York, 1981), p. 215.
- ²⁰J. Lin and N. Giordano, *Phys. Rev. B* **35**, 1071 (1987).
- ²¹E. Abrahams, P. W. Anderson, P. A. Lee, and T. V. Ramakrishnan, *Phys. Rev. B* **24**, 6783 (1981).
- ²²H. Fukuyama and E. Abrahams, *Phys. Rev. B* **27**, 5976 (1983).
- ²³W. E. Lawrence and A. B. Meador, *Phys. Rev. B* **18**, 1154 (1978).
- ²⁴U. Mizutani, T. B. Massalski, and J. Bevk, *J. Phys. F* **6**, 1 (1976).
- ²⁵E. N. Economou, in *Metal Hydrides* (Ref. 19), p. 1.
- ²⁶D. A. Papaconstantopoulos, B. M. Klein, E. N. Economou, and L. L. Boyer, *Phys. Rev. B* **17**, 141 (1978).
- ²⁷R. Meservey and P. M. Tedrow, *Phys. Lett. A* **58**, 131 (1976).
- ²⁸A. A. Abrikosov and L. P. Gorkov, *Zh. Eksp. Teor. Fiz.* **42**, 1088 (1962) [*Sov. Phys. JETP* **15**, 752 (1962)].
- ²⁹S. Geier, G. Bermann, N. Papanikolaou, N. Stefanou, and P. H. Dederichs, *Solid State Commun.* **87**, 471 (1993).
- ³⁰E. Wicke and H. Brondowsky, in *Hydrogen in Metals*, edited by G. Alefeld and J. Völkl, *Topics in Applied Physics* Vol. 29 (Springer-Verlag, Berlin, 1978), p. 73.
- ³¹R. Huguernin, G. P. Pells, and D. N. Baldock, *J. Phys.* **1**, 281 (1971).
- ³²P. Monod, *J. Phys. Colloq.* **39**, C6-1472 (1978).
- ³³T. S. Rahman, J. C. Parlebas, and D. L. Mills, *J. Phys. F* **8**, 2511 (1978).
- ³⁴A. H. McDonald, *J. Phys. F* **12**, 2579 (1982).
- ³⁵F. M. Mueller, A. J. Freeman, J. O. Dimmock, and A. M. Furdyna, *Phys. Rev. B* **1**, 4617 (1970).
- ³⁶G. Alquie, A. Kreisler, and J. P. Burger, *J. Less-Common Met.* **49**, 97 (1976).